IEEE Access
Multidisciplinary | Rapid Review | Open Access Journal

Received 26 March 2024, accepted 3 April 2024, date of publication 8 April 2024, date of current version 15 April 2024.

Digital Object Identifier 10.1109/ACCESS.2024.3385991

RESEARCH ARTICLE

Power Quality Improvement in Commercial and Industrial Sites: An Integrated Approach Mitigating Power Oscillations

AUGUSTO MATHEUS DOS SANTOS ALONSO[1], (Member, IEEE), LUIS DE ORO ARENAS[2], JAKSON PAULO BONALDO[3], JOSE DE A. OLÍMPIO FILHO[2], FERNANDO PINHABEL MARAFÃO[2], (Member, IEEE), AND HELMO K. MORALES PAREDES[2], (Senior Member, IEEE)

[1]Department of Electrical and Computer Engineering, University of São Paulo (USP), São Carlos 13566-590, Brazil
[2]São Paulo State University (UNESP), Institute of Science and Technology of Sorocaba, Sorocaba 18087-180, Brazil
[3]Department of Electrical Engineering, Federal University of Mato Grosso (UFMT), Cuiabá 78060-900, Brazil

Corresponding author: Augusto Matheus dos Santos Alonso (augusto.alonso@usp.br)

This work was supported in part by São Paulo Research Foundation (FAPESP) under Grant 2022/15423-3 and Grant 2022/07811-3, in part by the National Council for Scientific and Technological Development (CNPq) under Grant 309297/2021-4, in part by the Pró-Reitoria de Pesquisa e Inovação (PRPI) through the University of São Paulo under Grant 2022.1.9345.1.2/(Centro 49000/49053), and in part by the Mato Grosso Research Foundation (FAPEMAT) under Grant FAPEMAT.0001047/2022.

ABSTRACT This paper introduces a novel control strategy for multifunctional grid-tied inverters in industrial/commercial power systems, aiming to address the compensation of instantaneous power oscillations. The proposed strategy is derived from the Conservative Power Theory, which offers the ability to extract and analyze oscillating power terms directly in the *abc* frame. To demonstrate the efficacy of the proposed strategy, simulation results are presented, considering a scenario with a three-phase multi-functional grid-tied inverter with an LCL filter operating in a laboratory scale prototype. The power system includes various types of loads, such as linear, non-linear, unbalanced loads and a three-phase induction motor with capacitive compensation. Simulation results show the effectiveness of the proposed strategy in coping with the active power dispatch provided by the inverter, concomitantly ensuring that the induction motor operates with constant torque, as well as that the industrial/commercial electric system operates with improved power quality. Furthermore, the proposed strategy is also validated by means of experimental results obtained from a 3.6 kVA inverter prototype. The experimental findings affirm that the compensation of the targeted oscillating power terms is successfully achieved. Such a validation underscores the practical viability of applying the proposed strategy to real-world scenarios.

INDEX TERMS Conservative power theory, induction motor, instantaneous power oscillations, multifunctional inverters, power factor, power quality.

I. INTRODUCTION

Power quality (PQ) is a relevant matter for consumers and electric utilities worldwide, and its importance has been elevated since the past decades due to the widespread interconnection of electronic devices (e.g., loads - computers, lighting systems, elevators, rotating machines, electric vehicles (EVs) chargers, etc. [1]). Such devices present a nonlinear characteristic intrinsic to their operation, degrading voltage and current waveforms that are ideally desired to be sinusoidal. As a consequence, power oscillations and resonance issues associated with the existence of asymmetrical and distorted voltage/current components have become major concerns, particularly to industrial and commercial power systems that present sensitive and expensive electric equipment [2], [3].

The associate editor coordinating the review of this manuscript and approving it for publication was Alon Kuperman.

The dense existence of nonlinear electric devices is harmful due to the fact that their operational behavior can contribute to the amplification of non-sinusoidal currents circulating within the power grid, which degrades PQ indexes to undesired levels, both from utilities' and commercial/industrial consumers' perspectives [4]. The major technical concerns related to poor PQ within such a scenario include excessive transformer heating, interference in communication systems, audible noise, malfunctioning of protection and measurement systems, and increased vibrations in electric machines [5]. Moreover, it is worth highlighting that the interaction between harmonic currents and the feeder's impedance also causes non-sinusoidal voltage drops, distorting the voltages at the point of common coupling (PCC) [6]. Consequently, such a voltage behavior adversely affects the operation of induction motors, which are devices widely used in commercial/industrial sites, causing additional electric losses and, above all, torque pulsations [7], [8]. Moreover, low power factor is also evidenced as another cause deteriorating the performance of such machines [9]. Another relevant point is the incorporation of new and atypical loads into the electrical system, such as EV charging stations, which introduce operational challenges such as equipment malfunction and waveform distortion during the charging process, resulting in PQ degradation [10].

In the literature, the traditional and most economically viable solution for power factor correction and harmonic mitigation in commercial/industrial sites is typically accomplished by means of passive filters and capacitor banks [11], [12]. However, such a strategy is highly sensitive to the grid's impedance features, being associated with the rising of harmonic resonances when not properly designed. In addition, the main disadvantage of using passive filters and capacitor banks lies in their lack of dynamic adjustment for compensation. Once designed and installed, passive compensators cannot be easily adjusted to cope with changes in the voltage and current patterns of the grid [13].

On the other hand, solutions based on active filtering techniques have gained popularity over the past decades [14], [15], [16], [17]. The reason behind that trend is mostly due to the constant reduction in the prices related to such equipment, as well as the proliferation and flexibility of power electronic converters (PECs) associated with distributed energy resources (DERs), such as photovoltaic-(PV), fuel cell, battery and wind-based systems [18]. Considering the high investment and operating costs of additional devices in the installation aimed at improving power quality, the remaining capacity of the PECs has attracted significant interest, emerging as a promising solution to address such obstacles [3].

Consequently, several compensation strategies have been proposed in the literature to combine reactive, harmonic, and imbalance compensation [19], [20], [21], [22], [23], [24], [25], [26], [27] through the control setting of PECs. Nonetheless, despite the widespread use of PV and wind energy systems, PECs usually end up being underutilized due to the intermittency of such sources [19], [25]. To cope with that and meet cost-benefit reasonable alternatives, hybrid solutions that combine features of passive and active solutions can be employed to increase the utilization rate of PECs. For example: passive filters can be combined with active power filters (APFs); Static Var Compensator (SVC) is used in parallel with APF; SVC is associated with Static Synchronous Compensator (STATCOM); and others [23].

As shown in [24], an effective solution for harmonic mitigation and reactive compensation is the combination of active and passive filters, since it allows to reduce the overall investment while attaining satisfactory filtering performance. In [26], power factor correction is addressed by using traditional capacitor banks together with PV-based Multi-Functional Grid-Tied Inverters (MFGTI), and a study on the effects of installing a photovoltaic plant in an industrial environment is conducted. In [27], the use of a MFGTI is proposed for power factor compensation through synergistic control of capacitive reactive power. Power factor correction based on PECs and capacitor banks is also explored in [28], having reactive compensation as main goal, although neglecting the analysis of possible harmonic resonances.

In [2], a power factor correction strategy addressing harmonic resonance in different demand conditions is presented. Nonetheless, [2], as well as none of the works cited above, address the mitigation of oscillating power components, which can drastically reduce the lifespan of induction motors and deteriorate PQ of the industrial/commercial site.

Regarding the compensation of power oscillations, important findings related to the topic have been addressed in previous studies. In [29], the performance and applicability of compensation algorithms for switched compensators using the p-q theory are evaluated. The authors emphasize the oscillation of instantaneous real power, which can cause oscillating torques or frequency variations in weak systems, such as energy microgrids. They suggest that the oscillating portion of instantaneous real power arises from the connection of different types of low-inertia or non-controllable generators in the microgrid. However, this methodology does not explore scenarios involving the inverter's multifunctionality. In [30] and [31], an approach based on the Conservative Power Theory (CPT) is proposed to identify oscillatory components of instantaneous power in three-phase systems. The authors present an initial study to define reference signals for compensation of oscillating instantaneous power and active power injection in three-phase systems. They explore the use of the MFGTI to inject power into the grid and act as an APF, providing that the PEC does not exceed its nominal capacity.

A multifunctional inverter integrated with a Battery Energy Storage System (BESS) is proposed in [32]. The inverter includes a management strategy aimed at active power injection and reactive power compensation, taking into account the state of charge (SoC) of the BESS and PV intermittency. In [33], an energy management algorithm based on an MFGTI with BESS was developed, considering the optimal

system operation mode as well as selective disturbance compensation. However, the integration of BESS into the inverter system, as in [32] and [33], results in additional costs, making the system more expensive. In [34] proposes an efficient active and reactive power management scheme via fuel cell grid connection aiming at power factor correction; however, it does not address harmonic mitigation. A hybrid PV-battery system that performs multifunctional operations utilizing a grid-connected inverter is introduced in [35]. A multifunctional system integrating PV, battery, and APF, with metaheuristic tuning, has been proposed in [36]. However, neither [35] nor [36] investigates selective compensation and requires coordinate transformation and phase-locked loops (PLL) to generate reference currents for the inverter.

Considering that [29], [30], and [31] does not address the integration of the MFGTI with passive compensation solutions, it can be highlighted that the main contribution of this article lies in proposing a methodology related to the association of a capacitive bank and a MFGTI, resulting in a hybrid method enabling reactive compensation through these devices. This approach BC is used for reactive power compensation in the fundamental component and avoids the need to install new passive structures and their redundancy in the facilities, which are susceptible to resonance, increased costs, among other issues. Furthermore, the proposed strategy would allow for the adaptation and updating of the control structure of the MFGTI with a flexibility in the injection of active power, compensation of residual reactive power, and the mitigation of power and energy oscillations, thus ensuring a constant torque for electrical machines. A summary of the literature review concerning the comparison between the proposed control strategy and some state-of-the-art control strategies of multifunctional inverters and hybrid method for power quality improvement is presented in Table 1.

TABLE 1. Comparison between proposed control strategy and some state-of-the-art control strategies.

Reference	MFGTI	Flexibility	Method Hybrid	Cost
[11]	NO	NO	No	Low
[17], [24]	NO	NO	Yes	Medium
[19], [21], [22], [25], [27]	YES	YES	NO	Medium
[3], [20], [23]	YES	YES	YES	Higher
[30], [31]	YES	YES	NO	Medium
[32], [33]	YES	YES	YES	Higher
[35], [36]	YES	NO	YES	Higher
PROPOSED METHOD	**YES**	**YES**	**YES**	**Medium**

This paper proposes an approach capable of integrating a MFGTI with capacitor banks, additionality considering the perspective of having such equipment installed in industrial/commercial environments (e.g., shopping centers or industrial sites). Hence, the integrated approach allows to minimize oscillatory torque in three-phase induction motors and improve the power quality in industrial/commercial power systems. In the proposed integrated compensation system, the capacitor bank allows to compensate the power factor of a three-phase induction motor. On the other hand, the MFGTI is responsible for injecting active power, simultaneously mitigating oscillatory instantaneous power according to the conditions imposed by the industrial/commercial electric system. Whenever necessary, the MFGTI can also compensate for the remaining reactive power (i.e., the portion not compensated by the capacitor bank), always respecting the PEC's nominal capacity. Thus, the full potential of the industry microgrid's, the capacitive bank (CB), and the distributed energy resource (DER) can be exploited, only requiring the need for a firmware update of the inverter.

The proposed approach has the potential to increase the utilization of MFGTI in the industrial and commercial sectors, resulting in greater electricity savings and stronger reliability for the power supply. Additionally, it improves PQ and increases the lifespan of induction motors (IMs), since the MFGTI supports the compensation pulsating torques resulting from the intermittent nature of renewable energy sources, as well as from load imbalances, voltage imbalances, and harmonic components present in industrial/commercial installations. In this way, it ensures constant instantaneous power during the operation of IMs and other rotating machines in general.

II. PROPOSED COMPENSATION SYSTEM STRATEGY

An overview of a typical industrial electrical system connected to the grid is presented in Fig. 1, consisting of a DER represented by non-dispatchable generation source (e.g., PV-based source) responsible for supplying energy. Such a system includes a three-phase voltage source inverter (i.e., PEC) with current-controlled output, a CB for passive power factor compensation, line impedances, and a set of local loads. The coupling of the inverter with the main grid is achieved through an LCL filter, which ensures current and voltage waveforms are practically free of high-frequency ripples. Additionally, the presence of inductance L_2 enhances the system's robustness against variations in the grid impedance, which is usually unknown and can vary with time [37].

The industrial load consists of an induction motor (IM) with a CB (C_{Cap}), a balanced linear load (L_B and R_B), an unbalanced load (L_U and R_U), and non-linear load (R_N, L_N and C_N). It is important to note that a mechanical load (ML) is coupled to the shaft of the IM, with a rated power of 14.8 kW, torque of 74 N.m, and a power factor of 0.87. Note

TABLE 2. Parameters of the MFGTI and proposed system in computational simulation.

Parameter	Value	Parameter	Value
V_{Grid}^{Line}	460 V / 60 Hz	R_G, L_G	0.08Ω, 0.315 mH
P_{DER}	15 kW	R_1, L_1	10 mΩ, 0.5 mH
P_{IM}	14.8 kW	R_2, L_2, C_0	10 mΩ, 0.5 mH, 3.3 µF
V_{IM}	460 V	R_Z, L_Z	0.28 Ω, 1.1 mH
$PF_{IM} = \lambda_{IM}$	0.87	R_U, L_U	9 Ω, 18 mH
T_{IM}	74 N.m	R_B, L_B	30 Ω, 70 mH
C_{Cap}	55.4 µF	L_N, R_N, C_N	1 mH, 33 Ω, 780 µF,

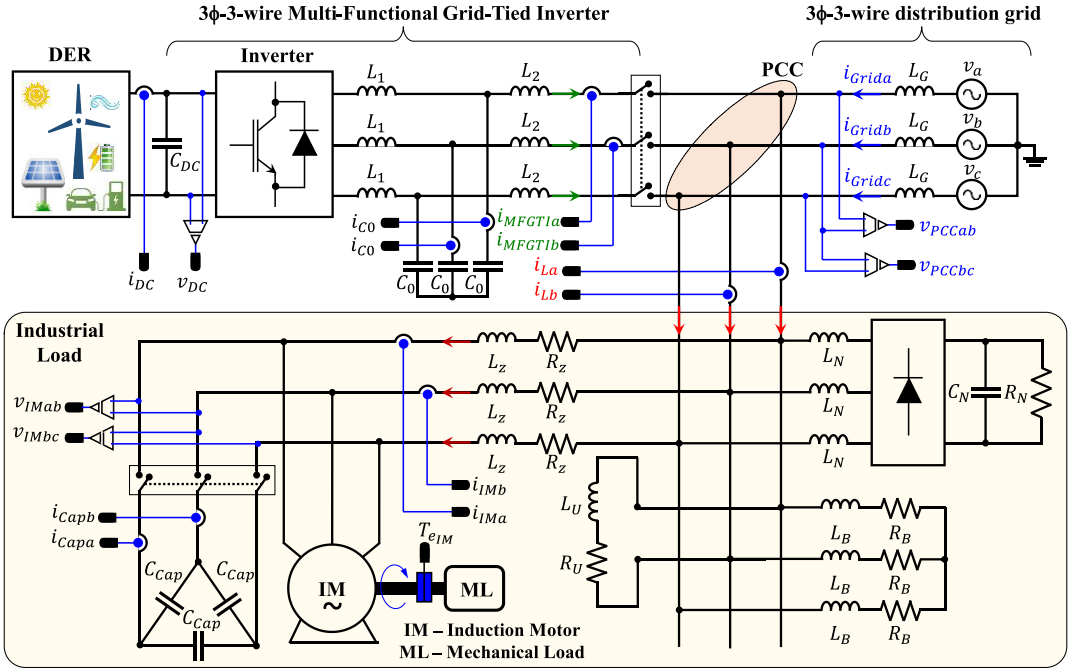

FIGURE 1. Interconnection of MFGTI to an industrial grid.

that, the power factor of the induction motor falls below the standardized index of 0.92, as stated in [38]. Table 2 shows the values of the main parameters adopted for the CB and MFGTI setup, as well as the characteristics of the electrical grid and loads. It is worth mentioning that the LCL filter was designed following [39], and the CB integrated with the three-phase squirrel cage induction motor was dimensioned to achieve a power factor of 0.95.

A. MFGTI CONTROL SYSTEM

The PEC's control algorithm is implemented in natural coordinates (*abc*). A simplified control system diagram is presented in Fig. 2, showing the generation of reference signals from the CPT and the control loops used. The modeling and design of the controllers are based on [40], [41], and [42]. The proposed control system utilizes two loops, with one loop dedicated to controlling the output current of the MFGTI (i_{MFGTI}) and another external loop responsible for maintaining a constant voltage at the DC bus (v_{CC}).

It's important to note that the system shown in Fig. 1 is a three-phase system with three wires. Thus, the current of phase *c*, is obtained by summing the currents of the MFGTI, i.e, $i_{MFGTIc} = -(i_{MFGTIa} + i_{MFGTIb})$, and the voltages are obtained from the line voltage, as described in [43].

The controller for the MFGTI's output current is based on a multi-resonant proportional controller [44], given by:

$$G_C(s) = K_C + \sum_{i=1,3,5} \frac{2K_{IPR}\omega_{CPR}s}{s^2 + 2\omega_{CPR}s + (h\omega_0)^2} \quad (1)$$

where h represents the harmonic order, ω_0 is the fundamental frequency of the grid, and K_C, K_{IPR}, ω_{CPR} correspond to the proportional gain, integral gain, and bandwidth of the resonant controller, respectively. The gain K_C of the current controller is calculated to ensure a certain cross-over frequency ω_C of the uncompensated open-loop transfer function, $OLTF_{nc}(s)$, as discussed in [37]:

$$K_C = \frac{1}{|OLTF_{nc}(\omega_C)|} \quad (2)$$

For the regulation of the DC bus voltage, a proportional-integral (PI) controller is adopted, designed according to [40]. To be aligned with the perspective of this paper, the regulator should operate with a sufficiently narrow bandwidth to avoid oscillations in the peak value of the current reference and minimize interaction with the current controller [37].

$$PI_{DC}(s) = K_{PDC} + \frac{K_{IDC}}{s} \quad (3)$$

Finally, the MFGTI was designed considering a switching frequency of 18 kHz due to the single update modulation strategy and physical design of the magnetic devices. Table 3 shows the values adopted for the current and voltage controllers.

TABLE 3. Parameters of current and voltage controllers.

Parameter	Value	Parameter	Value
K_C	2	K_{PDC}	5
K_{IPR}	100	K_{IDC}	50
ω_{CPR}	6.28 rad/s	ω_0	377 rad/s

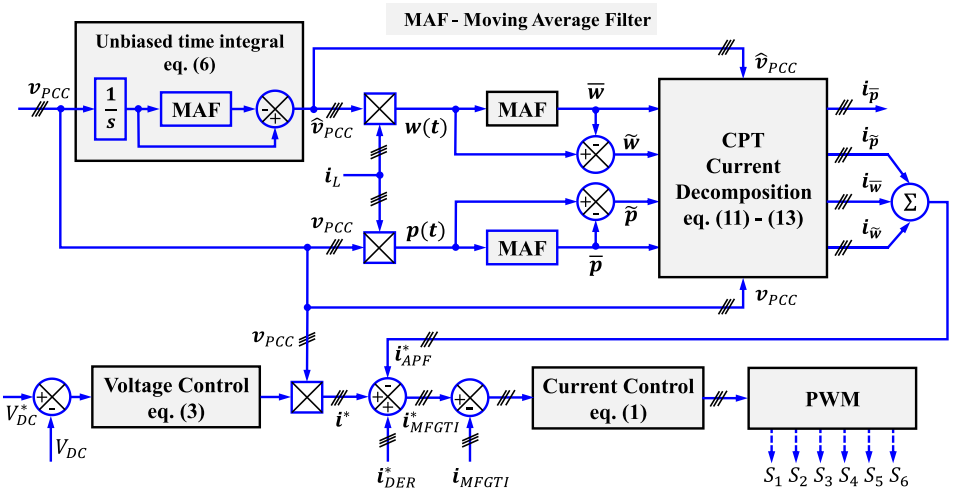

FIGURE 2. Control system and reference signals generation for proposed MFGTI.

The bandwidth of the current loop was set at 1.2 kHz aiming the compensation of current harmonics and phase margin in 45°. The bandwidth of the PI compensator for the DC bus voltage is adjusted to 7 Hz, and the phase margin to 70° in order to achieve a compensated system with low overshoot in order to maintain a voltage of 400 V at the DC bus. A detailed explanation about the complete process of modeling and design of the controllers is available in [40].

III. FOUNDATIONS FOR DECOMPOSITION OF OSCILLATORY POWER COMPONENTS

The decomposition of instantaneous power considered in this paper is based on average and oscillatory components, taking the CPT as a framework for such a task [45]. The CPT, which is an approach defined in time domain, is applicable to any periodic signal, enabling the analysis of both single-phase and multi-phase electrical systems. The CPT decomposes current and power signals into orthogonal components, yielding physically meaningful quantities without the need for PLL or coordinate transformations.

Due to the decoupling between the obtained current components, the CPT has proven to be an effective tool for generating reference signals to compensate disturbances in APF [43], MFGTI [19], [21], [25], [41] and microgrids [15], [27], [31]. A few applications can be found in [46]. The CPT defines two conservative quantities known as instantaneous power, $p(t)$, and instantaneous reactive energy, $w(t)$ [45]. The former is given by the dot product of voltage and current vectors, as shown in (4). On the other hand, $w(t)$ utilizes the vector of the unbiased time integral of voltages ($\hat{v}_m$) and the vector of current as shown is (5). Further details regarding the CPT and its main quantities are discussed in [45].

The definition of $\hat{v}_m$ is presented in (6), in which m represents the phases a, b and c, respectively.

$$p(t) = \begin{bmatrix} v_a & v_b & v_c \end{bmatrix} \cdot \begin{bmatrix} i_a \\ i_b \\ i_c \end{bmatrix} \tag{4}$$

$$w(t) = \begin{bmatrix} \hat{v}_a & \hat{v}_b & \hat{v}_c \end{bmatrix} \cdot \begin{bmatrix} i_a \\ i_b \\ i_c \end{bmatrix} \tag{5}$$

$$\hat{v}_m = \int_0^t v_m(\tau) d\tau - \frac{1}{T} \int_0^T \left[\int_0^t v_m(\tau) d\tau \right] dt \tag{6}$$

Observe that, the second term in (6) represents the average value of the voltage over a period (T). Moving Average Filters (MAF) are employed to calculate the average values of $p(t)$ and $w(t)$ as shown in (7) and (8), respectively, yielding the active power, P, and the reactive energy, W.

$$\bar{p}(t) = \frac{1}{T} \int_0^T p(t)\, dt = P \tag{7}$$

$$\bar{w}(t) = \frac{1}{T} \int_0^T w(t)\, dt = W \tag{8}$$

Similarly, to the p-q theory [47], the terms $p(t)$ and $w(t)$ defined in (4) and (5) can be decomposed into average and oscillatory components, as shown in (9) and (10), respectively. In the notation used, "$\sim$" represents the oscillating components of each term, while "$-$" indicates the average components.

$$p(t) = \bar{p} + \tilde{p} \tag{9}$$

$$w(t) = \bar{w} + \tilde{w} \tag{10}$$

Note that, the average and oscillatory components are valid regardless of the voltage and current waveforms. This characteristic makes the application of this methodology valid for both sinusoidal and non-sinusoidal voltage conditions. Moreover, the instantaneous power, $p(t)$, represents the useful energy per unit of time flowing from the source to the load or from the load to the source if negative. On the other hand, the average component, $\bar{p}$, consists of the energy per unit of time transferred from the source to the load (useful power). Meanwhile, the oscillatory component, $\tilde{p}$, undoubtedly has a zero average value and corresponds to the energy per unit of time exchanged between the source and the load. However,

at each instant, it represents an amount of energy that flows in the electrical circuit due to some type of undesirable current, caused by harmonics (usually due to uncommonly harmonic orders existing in voltages and currents) and imbalances present in the voltages and/or currents.

A similar procedure can be used to understand the components associated with reactive energy, $w(t)$. The average value, $\bar{w}$, corresponds to the average reactive power, arising from energy storage elements in the network or circuits without energy storage capability, which are responsible for the phase shift between voltages and currents. The oscillatory component, $\tilde{w}$, originates from harmonic components uncommonly existing in unbiased voltages integrals and currents, as well as imbalances associated with the flow of reactive energy in the electrical grid.

Works such as [29], [47], and [48] have demonstrated methods to compensate for oscillatory power components to achieve constant power in the grid side using p-q theory. However, these studies applied such concepts solely to APF and presented a trade-off between obtaining constant power and the resulting current waveform in the electrical grid. Nonetheless, the application of CPT for compensating oscillating power by means of MFGTI in industrial/commercial systems remains unexplored, necessitating in-depth studies on validation and applicability. Moreover, there is gap in the literature related to the application of such an approach when alongside CBs: requiring further studies to assess if this collaborative operation ensures the smooth and efficient working of industrial/commercial systems. Therefore, the primary objective of the upcoming sections is to address this gap and explore the potential of CPT in such applications.

A. REFERENCE SIGNALS FOR APF FUNCTION TO POWER QUALITY IMPROVEMENT

With the instantaneous power and reactive energy terms defined in (9) and (10), two instantaneous current components can be defined, namely instantaneous active ($\boldsymbol{i}_p$) and reactive

($\boldsymbol{i}_w$) currents:

$$\boldsymbol{i}_p(t) = \boldsymbol{i}_{\bar{p}} + \boldsymbol{i}_{\tilde{p}} = \frac{\bar{p}}{v_{abc}^2}\begin{bmatrix} v_a \\ v_b \\ v_c \end{bmatrix} + \frac{\tilde{p}}{v_{abc}^2}\begin{bmatrix} v_a \\ v_b \\ v_c \end{bmatrix} \tag{11}$$

$$\boldsymbol{i}_w(t) = \boldsymbol{i}_{\bar{w}} + \boldsymbol{i}_{\tilde{w}} = \frac{\bar{w}}{\hat{v}_{abc}^2}\begin{bmatrix} \hat{v}_a \\ \hat{v}_b \\ \hat{v}_c \end{bmatrix} + \frac{\tilde{w}}{\hat{v}_{abc}^2}\begin{bmatrix} \hat{v}_a \\ \hat{v}_b \\ \hat{v}_c \end{bmatrix} \tag{12}$$

where $v_{abc}^2 = v_a^2 + v_b^2 + v_c^2$ and $\hat{v}_{abc}^2 = \hat{v}_a^2 + \hat{v}_b^2 + \hat{v}_c^2$ are the instantaneous collective values of voltages and their unbiased time integral values, respectively, with the bold variables defined as vectors. Notice that the current vectors associated with the instantaneous terms $p(t)$ and $w(t)$ can be decomposed into two subcomponents, the average components ($\boldsymbol{i}_{\bar{p}}$ and $\boldsymbol{i}_{\bar{w}}$) and the oscillatory components ($\boldsymbol{i}_{\tilde{p}}$ and $\boldsymbol{i}_{\tilde{w}}$). The terms $\boldsymbol{i}_{\tilde{p}}$ and $\boldsymbol{i}_{\tilde{w}}$ represent the contributions of harmonic components and/or current imbalances that drive the oscillation in instantaneous power and energy, along with introducing additional losses within the power system.

It should be noted that from the load's perspective, the decomposed components in (11) and (12) do not represent any specific characteristics of the load behavior. Only under conditions of sinusoidal and balanced voltage, $\boldsymbol{i}_{\bar{p}}$ and $\boldsymbol{i}_{\bar{w}}$ coincide with the originally defined balanced active and reactive currents by CPT [45].

As the oscillatory component ($\boldsymbol{i}_{\tilde{p}}$) does not contribute to active power (P), the compensation reference signals can be expressed as the sum of $\boldsymbol{i}_{\bar{w}}$, $\boldsymbol{i}_{\tilde{p}}$ and $\boldsymbol{i}_{\tilde{w}}$, as illustrated in (13). It is worth noting that this compensation reference signals can be selectively applied, where the sum of the oscillatory components ($\boldsymbol{i}_{\tilde{p}} + \boldsymbol{i}_{\tilde{w}}$) is linked to the oscillation, while $\boldsymbol{i}_{\bar{w}}$ is associated with the flow of reactive power within the system.

$$\boldsymbol{i}_{comp} = \boldsymbol{i}_{\bar{w}} + \boldsymbol{i}_{\tilde{p}} + \boldsymbol{i}_{\tilde{w}} = \boldsymbol{i}_{APF} \tag{13}$$

From (13), the oscillatory components ($\boldsymbol{i}_{\tilde{p}}$ and $\boldsymbol{i}_{\tilde{w}}$) and $\boldsymbol{i}_{\bar{w}}$ can be independently compensated by a MFGTI (APF function) or even by combining a CB to compensate $\boldsymbol{i}_{\bar{w}}$ (partial or total) and MFGI to compensate $\boldsymbol{i}_{\tilde{p}} + \boldsymbol{i}_{\tilde{w}}$. Therefore, since the main objective of this work is to obtain constant instantaneous power (compensate for oscillations), the sum of the oscillatory components, $\boldsymbol{i}_{\tilde{p}} + \boldsymbol{i}_{\tilde{w}}$, will be considered as the reference.

B. REFERENCE SIGNALS FOR DER FUNCTION TO INJECT ACTIVE POWER

In this work, the Sinusoidal Current Synthesis (SCC) strategy [21], [49] is employed to feed the DER generated power into the grid. According to the SCC approach, the injected current waveform should match the fundamental positive-sequence component of the voltage at the point of interconnection, as seen in eq. (14).

$$\boldsymbol{i}_{DER} = \frac{P_{DER}}{\left(\boldsymbol{V}_1^+\right)^2}\begin{bmatrix} v_{1a}^+ \\ v_{1b}^+ \\ v_{1c}^+ \end{bmatrix} \tag{14}$$

where, $\left(\boldsymbol{V}_1^+\right)^2 = \left(V_{1a}^+\right)^2 + \left(V_{1b}^+\right)^2 + \left(V_{1c}^+\right)^2$ is the collective RMS value of the fundamental positive-sequence component of the voltages, and P_{DER} (15) represents the net power generated by the DER that needs to be injected into the electrical grid.

$$P_{DER} = \frac{1}{T}\int_0^T v_{DC}(t)\, i_{DC}(t)dt \tag{15}$$

C. REFERENCE SIGNAL GENERATION TO MFGTI

Based on the reference signals for compensation ($\boldsymbol{i}_{APF}$) and active power injection into the grid ($\boldsymbol{i}_{DER}$), the current reference, denoted as $\boldsymbol{i}_{MFGTI}$, is defined. This reference current will be synthesized by the multifunctional active power injection and compensation system, and its expression is as follows:

$$\boldsymbol{i}_{MFGTI} = \boldsymbol{i}_{DER} - \boldsymbol{i}_{APF} = \boldsymbol{i}_{DER} - \boldsymbol{i}_{\bar{w}} - (\boldsymbol{i}_{\tilde{p}} + \boldsymbol{i}_{\tilde{w}}) \tag{16}$$

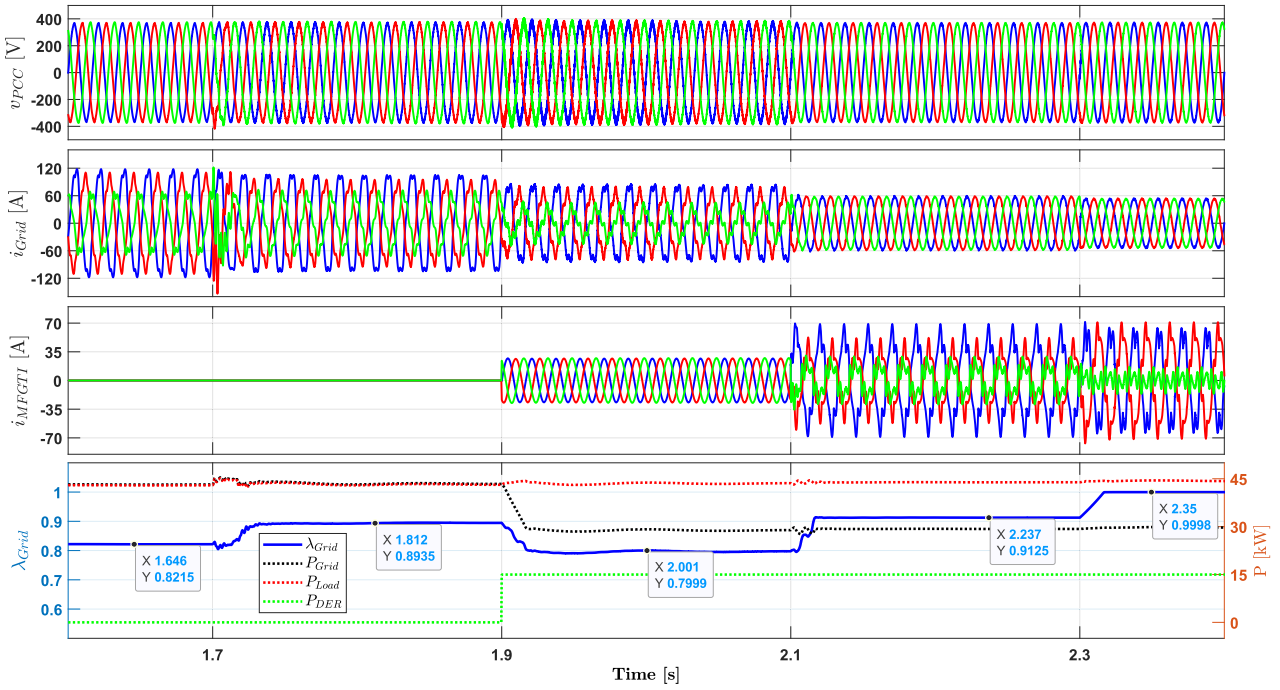

FIGURE 3. Waveforms of voltage, currents, active powers and power factor considering different compensation objectives.

From the perspective of integrating the MFGTI into commercial or industrial systems where traditional compensation systems like CB are already installed, compensation efforts can be divided in various ways. For instance, to enhance the operational flexibility of the MFGTI, the reference current, which is now to be synthesized by the combined MFGTI and CB system, results:

$$\boldsymbol{i}_{ref} = \boldsymbol{i}_{MFGTI} + \boldsymbol{i}_{CB} = \boldsymbol{i}_{DER} - \boldsymbol{i}_{APF} - \boldsymbol{i}_{CB} \tag{17}$$

where, the average reactive current component ($\boldsymbol{i}_{\bar{w}}$), associated with reactive energy (reactive power), can be compensated through cooperation between MFGTI and CB:

$$\boldsymbol{i}_{\bar{w}} = \boldsymbol{i}_{\bar{w}\_APF} + \boldsymbol{i}_{\bar{w}\_CB} \tag{18}$$

In this manner, the current reference for MFGTI is rewritten as:

$$\boldsymbol{i}_{MFGTI} = \boldsymbol{i}_{DER} - \boldsymbol{i}_{\bar{w}\_APF} - (\boldsymbol{i}_{\tilde{p}} + \boldsymbol{i}_{\tilde{w}}) \tag{19}$$

where, $\boldsymbol{i}_{\bar{w}\_APF}$ represents the residual reactive current, that which CB does not compensate.

Hence, the current reference generation structure enables the synthesis of the reference signal to compensate for oscillating torque in rotating machines ($\boldsymbol{i}_{\tilde{p}} + \boldsymbol{i}_{\tilde{w}}$) by the MFGTI, while reactive power ($\boldsymbol{i}_{\bar{w}}$) is compensated by the CB. However, in real industrial and commercial electrical systems, power factor correction is typically based on limits set by standards and/or regulatory guidelines.

Therefore, it is common to design the CB to correct the power factor, for example, to 0.92. In this scenario, the remaining reactive power that is not compensated by the CB would be complemented by the MFGTI, as indicated in equation (19). Furthermore, $\boldsymbol{i}_{\bar{w}\_APF}$ enables dynamic reactive power compensation, in contrast to the almost static function performed by the CB, ensuring greater dynamism and flexibility in enhancing the power quality of industrial/commercial electrical systems.

IV. SIMULATION RESULTS

The computational simulation of the system shown in Fig. 1 is conducted in this section with the aim of demonstrating the flexibility of the compensation system proposed in this work and to showcase the effectiveness of compensating power oscillations, resulting in reduced torque oscillations for induction motors widely used in industrial and commercial systems. The system and controller parameters simulated are presented in Table 2 and Table 3. The simulation results are discussed in terms of voltage and current waveforms at the PCC and at the IM's connection point, as shown in Fig. 3 and Fig. 4.

At $t < 1.7$ s, the system operates without any compensation, as observed in Fig. 3 and Fig. 4, with a low power factor at the grid ($\lambda_{Grid} = 0.82$) and highly unbalanced and distorted current in the grid (i_{Grid}). The IM operates with an initial power factor ($PF_{IM} = \lambda_{IM} = 0.87$) and exhibits fluctuations in instantaneous power, as well as torque oscillations.

For $t > 1.7$ s, the CB is connected to the terminals of the IM. In this situation, as expected, the power factor at the IM terminals converges to the desired value, i.e., $\lambda_{IM} = 0.95$. Consequently, the power factor measured at the PCC also improves, converging to $\lambda_{Grid} = 0.89$. However, observed that, the current at the IM terminals becomes more distorted

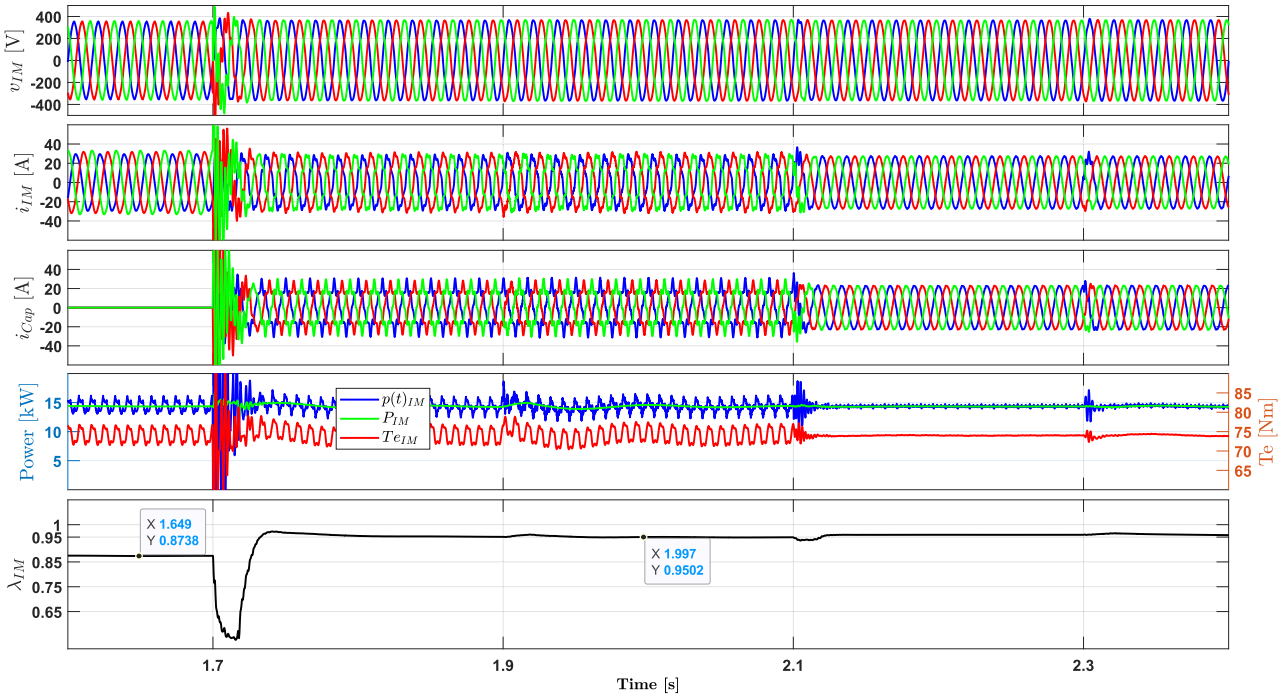

FIGURE 4. Waveforms of voltage, currents, active power, instantaneous power, torque and power factor at the connection point of the IM.

due to the interaction with the CB and the harmonics imposed by the non-linear load.

At $t > 1.9$ s, the MFGTI initiates its operation by injecting only active power into the grid. Note that the inverter current (i_{MFGTI}) is sinusoidal, meaning that there is no disturbance compensation, resulting in the persistence of power and torque oscillations in the IM as well as the unbalanced and distortion current at the grid. With the injection of active power into the system, the net active power in the grid decreases, consequently the power factor in the grid, decreasing to, $\lambda_{Grid} = 0.80$.

At $t > 2.1$ s, the multifunctional operation of the MFGTI begins, with the activation of the current reference to compensate for oscillatory terms ($\tilde{p}$ e $\tilde{w}$). At this moment, the current reference for the MFGTI is given by $i_{MGTI} = i_{DER} - i_{\tilde{p}} - i_{\tilde{w}}$, while the CB contributes by compensating part of the reactive power seen by the grid ($i_{\tilde{w}} - i_{CB}$). Consequently, the current synthesized by the MFGTI (i_{MFGTI}) becomes highly distorted and unbalanced, as shown in Fig. 3, while the grid current (i_{Grid}) becomes sinusoidal and balanced, and the grid power factor increases to 0.91. On the other hand, Fig. 4 illustrates that, starting from point 3, due to the compensation of $\tilde{p}$ and $\tilde{w}$, the previously observed oscillation in instantaneous power ceases. Thus, the contribution of this work to the compensation of power oscillations is highlighted, resulting in constant torque in the IM.

Finally, at $t > 2.3$ s, reactive compensation is added, i.e., now the reference for the MFGTI is given by (19). Since the term $i_{\tilde{w}\_APF}$ encompasses the reactive current related to the remaining reactive demand of the system, the power factor in the grid increases from 0.91 to 1.0.

V. EXPERIMENTAL RESULTS

Experimental results are presented herein to validate the operation of a three-phase three-wire MFGTI that is capable of injecting active power into grid and compensating oscillating instantaneous power, aiming at improving power quality at the PCC. Fig. 5 depicts the electric circuit and

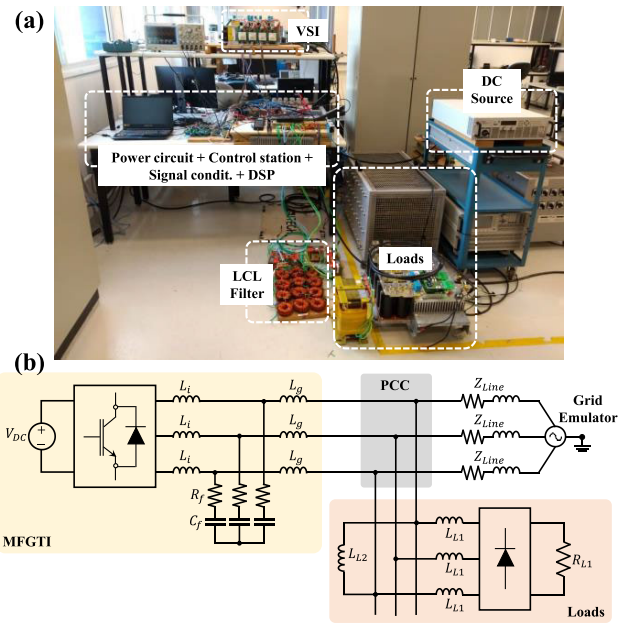

FIGURE 5. (a) An overview of the laboratory's small-scale experimental setup of MFGTI, (b) Schematic diagram of MFGTI connection to AC grid.

a picture of the laboratory-scale prototype assembled for the experiments. A three-leg topology using SEMIKRON SEMiX 403GB128Ds IGBT modules with Skyper 32PRO gate drivers was adopted for experiments, considering a 22.5 kVA grid-connected inverter. The detailed specifications considered for the grid, loads, line impedances cables connecting the grid to the PCC of the prototype and MFGTI during the experiments are shown in Table 4.

TABLE 4. Parameters of the experimental prototype.

Grid	
Nominal line-line voltage	220 V / 60 Hz
Line impedances (Z_{lines})	0.11+j10^{-3} Ω
Loads	
L_{L1}; R_{L1} ; L_{L2}	1 mH; 124.3 Ω; 40 mH
MFGTI	
DC-link voltage (V_{DC})	500 V
Rated Power/ DER	22.5 kVA/ 5 kW
$L_i = L_g$	1 mH,
C_f; R_f	2.2 µF; 1 Ω
Proportional gain (G_c(s)	K_C = 0.0401
Harmonic gain (G_c(s))	K_{IPR} = 15.63
Switching frequency (f_{sw})	18 kHz

In this prototype, a 30 kVA four-quadrant AC voltage source, REGATRON (model TC-ACS-30-528-4WR), emulates the power grid, and two loads are responsible for drawing power. One of the loads (i.e., L_1) is composed by a three-phase diode-bridge rectifier presenting inductors at the input terminals, consequently drawing active, reactive and harmonics currents from the grid. On the other hand, the second load (i.e., L_2) is single-phase connected and presents an inductive behavior, causing the circulation of unbalanced currents. Hence, by analyzing the power flow through the PCC (see Fig. 5), oscillating instantaneous powers are expected to be measured during the operation of this circuit. The measurement and data logging of voltages and currents are performed by a DPO3000 Tektronix oscilloscope, and MATLAB/Simulink® is also used to plot the results of the instantaneous active and reactive terms.

The prototype also comprises a MFGTI, which is composed of a voltage source inverter (VSI) having an *LCL* output filter with passive damping. A 5 kW DC voltage source is connected to the DC-link of the VSI to emulate the active power generation generated by a DER. A TMS320F28379D digital signal processor (DSP) is used to control the MFGTI and implement the current decomposition presented in Section III, which allows to compensate the oscillating powers. Proportional-resonant controllers [36], tuned at the fundamental and selected odd harmonic orders (i.e., 3rd up to 13th), are responsible for guaranteeing adequate tracking of the current references generated by the proposed approach. The following four main operational conditions are considered for the experiments carried out with the prototype:

- Scenario I: only the loads operate and the MFGTI is idle (i.e., not processing any currents);
- Scenario II: the MFGTI starts to operate by only injecting active power;
- Scenario III: besides providing active power injection, the $\tilde{p}$ and $\tilde{w}$ terms are compensated;
- Scenario IV: the MFGTI only compensates $\tilde{p}$ and $\tilde{w}$.

The experimental results for Scenario I are presented in Fig. 6, in which one can note the waveforms measured at the PCC for the line voltages (v_{PCC-ab} and v_{PCC-ca}) and the line currents (i_{PCC-a}, $i_{PCC-b}$and i_{PCC-c}). It is evident that, although the grid voltages are sinusoidal and balanced, the two loads draw currents that are distorted and unbalanced. Consequently, since the MFGTI is not operating and does not influence on the operation of the circuit, the instantaneous power $p\,(t)$ and reactive energy $w\,(t)$ present significant magnitudes. Moreover, the decomposition of the power components shown in Fig. 6 indicates that $\bar{p}$, $\bar{w}$, $\tilde{p}$and$\tilde{w}$ flow through the PCC. Note that these last two terms present significant amplitudes (i.e., approximately ± 3200 W and ± 10 J, respectively).

For Scenario II, the MFGTI is enabled, aiming at only processing at active power, similarly to the operation of a distributed generation system. Thus, 1600 W is injected into the grid, as demonstrated in Fig. 7 by the practically sinusoidal currents processed by the MFGTI. As a consequence, the PCC current waveforms slight change in relation to Scenario I. Most importantly, Fig. 7 shows that the term $\tilde{p}$ and the reactive energies, $\bar{w}$ and $\tilde{w}$ remained practically the same. However, the term $\bar{p}$ became negative (i.e., approximately -860 W), indicating that the active power provided by the MFGTI fed the loads and its exceeding quantity is dispatched to grid.

Now, during Scenario III, the multifunctional capability of the MFGTI is demonstrated. Fig. 8 shows the behavior

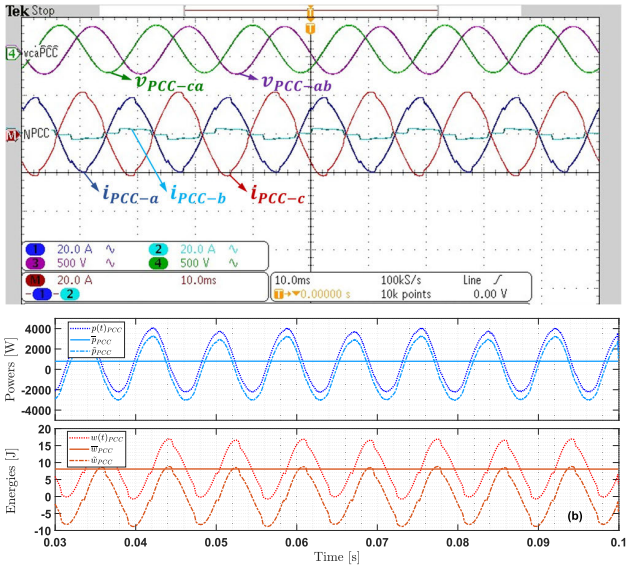

FIGURE 6. Voltage and current waveforms and instantaneous active and reactive terms for Scenario I (only loads connected to the PCC).

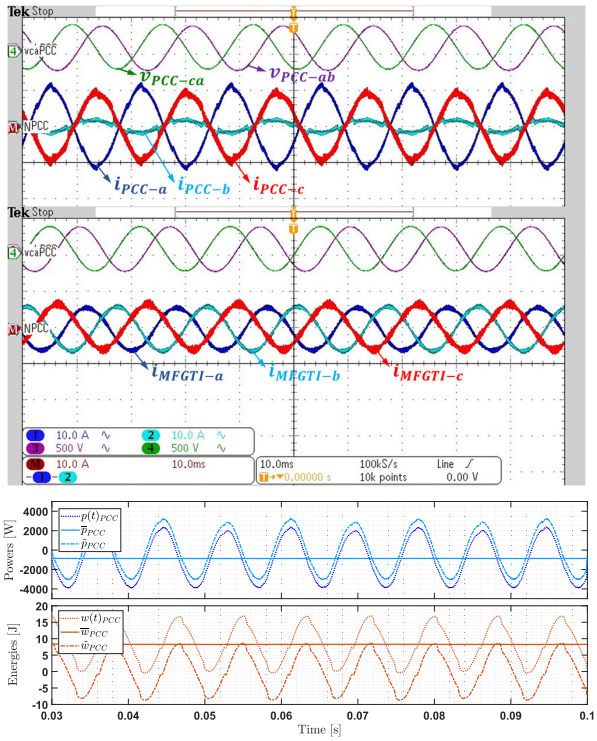

FIGURE 7. Voltage and current waveforms and instantaneous active and reactive terms for scenario II (MFGTI processing only active power).

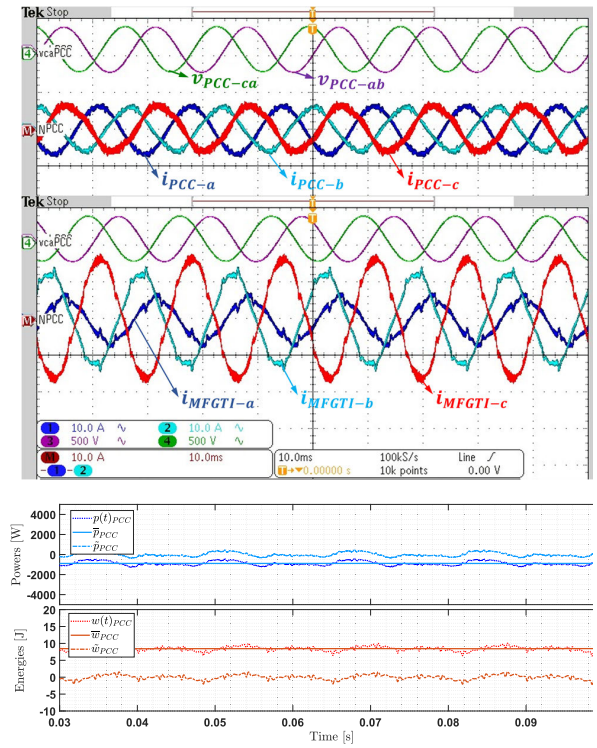

FIGURE 8. Voltage and current waveforms and instantaneous active and reactive terms for scenario II (MFGTI processing active power and $\tilde{p}$ and $\tilde{w}$ terms are compensated).

of the system when the compensation of $\tilde{p}$ and $\tilde{w}$ is added to operation of the MFGTI, while still injecting 1600 W of

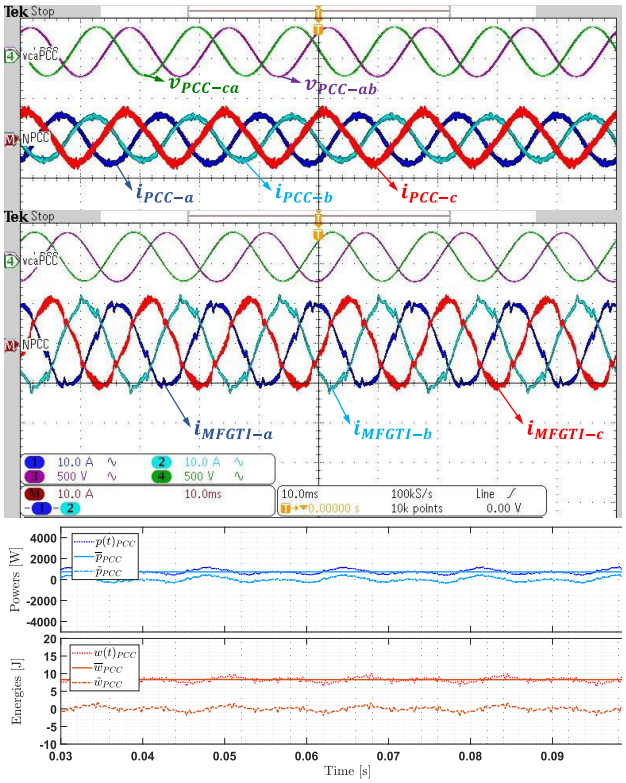

FIGURE 9. Voltage and current waveforms and instantaneous active and reactive terms for Scenario IV (MFGTI only addressing $\tilde{p}$ and $\tilde{w}$ compensation without any active power injection).

active power into the grid. Note that the MFGTI's currents are now distorted and unbalanced, consequently resulting in low-distorted and balanced currents at the PCC during steady state. Hence, such result proves that the MFGTI is capable of offering ancillary services concomitantly to the conversion of active power. Moreover, it is evident in Fig. 8 that the oscillations previously existing in the instantaneous active and reactive terms ($p(t)$ and $w(t)$) were significantly reduced. For instance, note that $\tilde{p}$ and $\tilde{w}$ now present maximum amplitudes close to $\pm$ 330 W and $\pm$ 1.5 J. Yet, the term $\bar{w}$ remained practically unchanged, which validates the feasibility of the compensation approach to real applications.

The last experiment depicted in Fig. 9 considers the MFGTI operating without having power being generated at its DC side (e.g., as an active filter). This case is presented to certify that the proposed power decomposition method is not only valid to MFGTIs, but it can also be applied for the operation of other power conditioners. Thus, during this experiment, the MFGTI injects no active power but compensates $\tilde{p}$and$\tilde{w}$. By doing that, the PCC again operates with low oscillations for $p(t)$ and $w(t)$ during steady state, although the grid is responsible for entirely supplying the loads with active and reactive power. One can, for example, note that $\bar{p}$ and $\bar{w}$ present practically the same amplitude as during Scenario I (see Fig. 6), resulting in PCC currents that are low-distorted and balanced, since the harmonic and unbalanced currents were practically mitigated by the MFGTI.

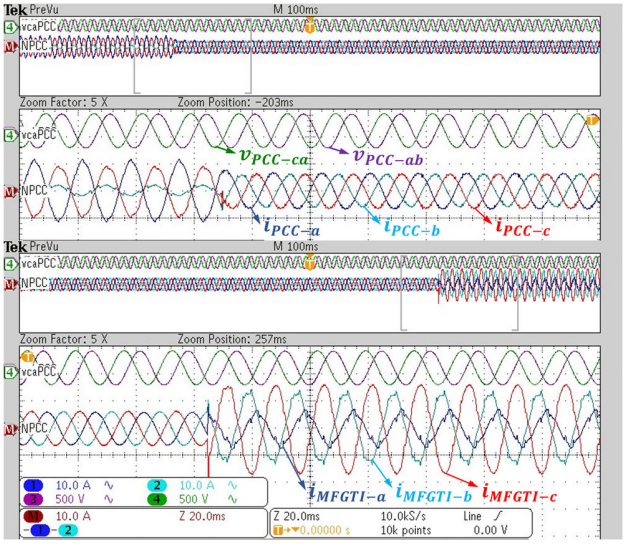

FIGURE 10. Experimental results demonstrating the transition from Scenario II to Scenario III.

Finally, an additional experimental result in presented in Fig. 10, aiming at demonstrating the dynamic behavior of the MFGTI while transiting from different operational scenarios. This result starts with the MFGTI operating as in Scenario II (i.e., only injecting active power), then transiting to Scenario III by adding the compensation of $\tilde{p}$ and $\tilde{w}$ to its current reference generation. This result proves that the MFGTI operation practically did not respond with any current or voltage spikes, and a smooth transition occurred between the operating modes. The same behavior can also be evidenced at the PCC, as the current smooth and quickly becomes practically sinusoidal and balanced. Hence, it is validated that the proposed compensation of oscillating power does not impact negatively the dynamic response of the MFGTI.

VI. CONCLUSION

This paper has introduced a novel strategy aimed at enhancing the power quality in industrial and commercial systems. The compensation system is based on the mean and oscillatory terms derived from the CPT. Experimental and simulation results have demonstrated that this proposed approach leverages grid-connected inverter infrastructure to inject active power while concurrently compensating for oscillatory terms in instantaneous power. This feature is of paramount importance in industrial and commercial sectors equipped with electric machines, such as induction motors, as the reduction in instantaneous power oscillations leads to a decrease in oscillating torque, thereby preventing their degradation and improper operation. This, in turn, contributes to preserves their lifespan, reducing losses, and minimizing heat generation of these and other equipment installed in industrial and commercial systems.

Furthermore, this paper has also shown that in industrial and commercial systems comprising both linear and nonlinear loads, as well as electric machinery, the integration of grid-connected multifunctional inverters with pre-installed capacitor banks for induction motor power factor correction can collaborate to minimizing the internal power losses and enhance the power quality of the electrical network. In the analyzed scenario, while the capacitor bank partially provides to the reactive power demand of the induction motor, the MFGTI injects active power, compensates for oscillations in instantaneous power, and still supplies the remaining reactive power demand of the industry or commerce. Thus, the flexibility introduced by the proposed control system enables collaborative operation between the capacitor bank and the MFGTI, instantly adjusting the power factor compensation level at the PCC to values exceeding those originally achievable with capacitor banks, for example.

It is worth noting that the proposed compensation of oscillating power not only avoids torque oscillation, but also minimizes both distortion and unbalance currents on the grid side, and increases the lifetime of electrical machines. On the other hand, separation of the oscillatory components, as in p-q power theory (or its derivatives), can be achieved by using low-pass filters. Consequently, there are delays in the compensation response when load variations are present.

Finally, future research activities principally intend to: i) validate the adequate operation of the proposed strategy under distorted voltage conditions; ii) address the methodology for four-wire systems; iii) expand the methodology by considering the separation of harmonic effects and imbalances, given that power and energy oscillations stem from such effects, as well as the consideration of DGs operating under limited power capability.

REFERENCES

[1] D. Lumbreras, E. Gálvez, A. Collado, and J. Zaragoza, "Trends in power quality, harmonic mitigation and standards for light and heavy industries: A review," *Energies*, vol. 13, no. 21, p. 5792, Nov. 2020, doi: 10.3390/en13215792.

[2] S. Lin, D. Salles, W. Freitas, and W. Xu, "An intelligent control strategy for power factor compensation on distorted low voltage power systems," *IEEE Trans. Smart Grid*, vol. 3, no. 3, pp. 1562–1570, Sep. 2012, doi: 10.1109/TSG.2012.2201756.

[3] K. Zhang, L. Wang, Y. Pang, S. Liao, X. Yang, and M.-C. Wong, "Power selective control with fault tolerance of multifunctional inverter for active power injection and power quality compensation," *IEEE Trans. Ind. Electron.*, vol. 70, no. 5, pp. 4309–4319, May 2023, doi: 10.1109/TIE.2022.3186357.

[4] A. Santos, G. P. Duggan, P. Young, S. Frank, A. Hughes, and D. Zimmerle, "Harmonic cancellation within AC low voltage distribution for a realistic office environment," *Int. J. Electr. Power Energy Syst.*, vol. 134, Jan. 2022, Art. no. 107325, doi: 10.1016/j.ijepes.2021.107325.

[5] D. Razmi, T. Lu, B. Papari, E. Akbari, G. Fathi, and M. Ghadamyari, "An overview on power quality issues and control strategies for distribution networks with the presence of distributed generation resources," *IEEE Access*, vol. 11, pp. 10308–10325, 2023, doi: 10.1109/ACCESS.2023.3238685.

[6] M. B. Arcadepani, D. T. Rodrigues, A. C. Moreira, J. P. Bonaldo, H. G. Júnior, and H. K. M. Paredes, "Conservative power theory for harmonic voltage responsibility assignment," *IEEE Latin Amer. Trans.*, vol. 20, no. 3, pp. 443–450, Mar. 2022, doi: 10.1109/TLA.2022.9667142.

[7] J. Policarpo G. de Abreu and A. E. Emanuel, "Induction motors loss of life due to voltage imbalance and harmonics: A preliminary study," in *Proc. 9th Int. Conf. Harmon. Quality Power*, Oct. 2000, pp. 75–80, doi: 10.1109/ICHQP.2000.897001.

[8] A. B. F. Neves, M. V. B. de Mendonça, A. de Leles Ferreira Filho, and G. Z. Rosa, "Effects of voltage unbalance and harmonic distortion on the torque and efficiency of a three-phase induction motor," in *Proc. 17th Int. Conf. Harmon. Quality Power (ICHQP)*, Oct. 2016, pp. 943–948, doi: 10.1109/ICHQP.2016.7783350.

[9] S. R. Nassar, A. A. Eisa, A. A. Saleh, M. A. Farahat, and A. F. Abdel-Gawad, "Evaluating the impact of connected non linear loads on power quality—A nuclear reactor case study," *J. Radiat. Res. Appl. Sci.*, vol. 13, no. 1, pp. 688–697, Jan. 2020, doi: 10.1080/16878507.2020.1828018.

[10] M. Inci and K. Ç. Bayındır, "Single-stage vehicular fuel cell system with harmonic elimination capability to suppress distortion effects of electric vehicle parking lots," *J. Power Sources*, vol. 597, Mar. 2024, Art. no. 234175, doi: 10.1016/j.jpowsour.2024.234175.

[11] G. Joksimovic, "Transformer reactive power compensation—Fixed capacitor bank calculation," *IEEE Trans. Power Del.*, vol. 30, no. 3, pp. 1629–1630, Jun. 2015, doi: 10.1109/TPWRD.2014.2373039.

[12] J. Dixon, L. Moran, J. Rodriguez, and R. Domke, "Reactive power compensation technologies: State-of-the-art review," *Proc. IEEE*, vol. 93, no. 12, pp. 2144–2164, Dec. 2005, doi: 10.1109/JPROC.2005.859937.

[13] S. Anwar, A. Elrayyah, and Y. Sozer, "Efficient single phase power factor improvement strategy for microgrid operation," in *Proc. IEEE Appl. Power Electron. Conf. Expo. (APEC)*, Mar. 2014, pp. 972–977, doi: 10.1109/APEC.2014.6803425.

[14] A. Kalair, N. Abas, A. R. Kalair, Z. Saleem, and N. Khan, "Review of harmonic analysis, modeling and mitigation techniques," *Renew. Sustain. Energy Rev.*, vol. 78, pp. 1152–1187, Oct. 2017, doi: 10.1016/j.rser.2017.04.121.

[15] A. C. Moreira, H. K. M. Paredes, W. A. de Souza, F. P. Marafão, and L. C. P. da Silva, "Intelligent expert system for power quality improvement under distorted and unbalanced conditions in three-phase AC microgrids," *IEEE Trans. Smart Grid*, vol. 9, no. 6, pp. 6951–6960, Nov. 2018, doi: 10.1109/TSG.2017.2771146.

[16] B. Singh, K. Al-Haddad, and A. Chandra, "A review of active filters for power quality improvement," *IEEE Trans. Ind. Electron.*, vol. 46, no. 5, pp. 960–971, Oct. 1999, doi: 10.1109/41.793345.

[17] B. Singh, V. Verma, A. Chandra, and K. Al-Haddad, "Hybrid filters for power quality improvement," *IEE Proc. Gener., Transmiss. Distrib.*, vol. 152, no. 3, p. 365, 2005, doi: 10.1049/ip-gtd:20045027.

[18] M. Inci, "A flexible perturb & observe MPPT method to prevent surplus energy for grid-failure conditions of fuel cells," *Int. J. Hydrogen Energy*, vol. 46, no. 79, pp. 39483–39498, Nov. 2021, doi: 10.1016/j.ijhydene.2021.09.185.

[19] H. K. M. Paredes, D. T. Rodrigues, J. C. Cebrian, and J. P. Bonaldo, "CPT-based multi-objective strategy for power quality enhancement in three-phase three-wire systems under distorted and unbalanced voltage conditions," *IEEE Access*, vol. 9, pp. 53078–53095, 2021, doi: 10.1109/ACCESS.2021.3069832.

[20] L. Wang, C.-S. Lam, and M.-C. Wong, "Analysis, control, and design of a hybrid grid-connected inverter for renewable energy generation with power quality conditioning," *IEEE Trans. Power Electron.*, vol. 33, no. 8, pp. 6755–6768, Aug. 2018, doi: 10.1109/TPEL.2017.2753838.

[21] F. P. Marafão, D. I. Brandão, A. Costabeber, and H. K. M. Paredes, "Multi-task control strategy for grid-tied inverters based on conservative power theory," *IET Renew. Power Gener.*, vol. 9, no. 2, pp. 154–165, Mar. 2015, doi: 10.1049/iet-rpg.2014.0065.

[22] J. P. Bonaldo, G. Schiavon, H. K. Morales Paredes, and J. A. Pomilio, "Multifunctional operation of current controlled VSI based on the harmonic content of PCC voltage," in *Proc. IEEE 8th Int. Symp. Power Electron. Distrib. Gener. Syst. (PEDG)*, Apr. 2017, pp. 1–6, doi: 10.1109/PEDG.2017.7972490.

[23] L. Wang, C.-S. Lam, and M.-C. Wong, "Multifunctional hybrid structure of SVC and capacitive grid-connected inverter (SVC//CGCI) for active power injection and nonactive power compensation," *IEEE Trans. Ind. Electron.*, vol. 66, no. 3, pp. 1660–1670, Mar. 2019, doi: 10.1109/TIE.2018.2838085.

[24] S. Vukojicic, S. Pavlovic, and L. Ristic, "Passive, active and hybrid filters as a part of the energy efficient electrical drives curriculum," in *Proc. 20th Int. Symp. Power Electron. (Ee)*, Oct. 2019, pp. 1–6, doi: 10.1109/PEE.2019.8923030.

[25] J. P. Bonaldo, V. A. De Souza, A. M. D. S. Alonso, L. D. O. Arenas, F. P. Marafão, and H. K. M. Paredes, "Adaptive power factor regulation under asymmetrical and non-sinusoidal grid condition with distributed energy resource," *IEEE Access*, vol. 9, pp. 140487–140503, 2021, doi: 10.1109/ACCESS.2021.3119335.

[26] L. S. Gusman, H. A. Pereira, J. M. S. Callegari, and A. F. Cupertino, "Design for reliability of multifunctional PV inverters used in industrial power factor regulation," *Int. J. Electr. Power Energy Syst.*, vol. 119, Jul. 2020, Art. no. 105932, doi: 10.1016/j.ijepes.2020.105932.

[27] H. K. Morales-Paredes, J. P. Bonaldo, and J. A. Pomilio, "Centralized control center implementation for synergistic operation of distributed multifunctional single-phase grid-tie inverters in a microgrid," *IEEE Trans. Ind. Electron.*, vol. 65, no. 10, pp. 8018–8029, Oct. 2018, doi: 10.1109/TIE.2018.2801780.

[28] P. Jintakosonwit, S. Srianthumrong, and P. Jintagosonwit, "Implementation and performance of an anti-resonance hybrid delta-connected capacitor bank for power factor correction," *IEEE Trans. Power Electron.*, vol. 22, no. 6, pp. 2543–2551, Nov. 2007, doi: 10.1109/TPEL.2007.909232.

[29] E. H. Watanabe, M. Aredes, J. L. Afonso, J. G. Pinto, L. F. C. Monteiro, and H. Akagi, "Instantaneous *p-q* power theory for control of compensators in micro-grids," in *Proc. Int. School Nonsinusoidal Currents Compensation*, Jun. 2010, pp. 17–26, doi: 10.1109/ISNCC.2010.5524475.

[30] J. de Arimatéia Olímpio Filho, H. K. M. Paredes, A. M. dos Santos Alonso, J. P. Bonaldo, F. P. Marafão, and M. G. Simões, "3-phase multi-functional grid-tied inverter for compensation of oscillating instantaneous power," in *Proc. IEEE 15th Brazilian Power Electron. Conf., 5th IEEE Southern Power Electron. Conf. (COBEP/SPEC)*, Dec. 2019, pp. 1–6, doi: 10.1109/COBEP/SPEC44138.2019.9065443.

[31] J. de Arimatéia Olímpio Filho, H. K. M. Paredes, J. P. Bonaldo, A. M. dos Santos Alonso, F. P. Marafão, and M. G. Simões, "Compensation of oscillating instantaneous power in modern microgrids based on the conservative power theory," *Eletrônica de Potência*, vol. 25, no. 3, pp. 261–271, Sep. 2020, doi: 10.18618/REP.2020.3.0017.

[32] L. H. Meneghetti, E. L. Carvalho, G. B. K. Schmidt, E. G. Carati, J. P. da Costa, C. M. de Oliveira Stein, Z. L. L. Nadal, and R. Cardoso, "Control strategy and power management for multifunctional inverters with BESS and reactive power compensation," in *Proc. IEEE 15th Brazilian Power Electron. Conf. 5th IEEE Southern Power Electron. Conf. (COBEP/SPEC)*, Dec. 2019, pp. 1–6, doi: 10.1109/COBEP/SPEC44138.2019.9065726.

[33] V. S. R. V. Oruganti, V. S. S. S. S. Dhanikonda, A. Mortezaei, T. D. C. Busarello, and M. G. Simões, "Power management algorithm for a conservative power theory battery storage based multi-functional three phase grid connected PV inverter," *Int. Trans. Electr. Energy Syst.*, vol. 30, p. e12605, no. 11, Nov. 2020, doi: 10.1002/2050-7038.12605.

[34] M. Inci, "Active/reactive energy control scheme for grid-connected fuel cell system with local inductive loads," *Energy*, vol. 197, Apr. 2020, Art. no. 117191, doi: 10.1016/j.energy.2020.117191.

[35] J. S. Dohler, L. F. da Rocha, D. C. Silva, P. M. de Almeida, A. A. Ferreira, and J. G. Oliveira, "Analysis and operation of a PV-battery system using a multi-functional converter," in *Proc. IEEE 15th Brazilian Power Electron. Conf. 5th IEEE Southern Power Electron. Conf. (COBEP/SPEC)*, Dec. 2019, pp. 1–6, doi: 10.1109/COBEP/SPEC44138.2019.9065801.

[36] R. Kumar, H. O. Bansal, and D. Kumar, "Improving power quality and load profile using PV-battery-SAPF system with metaheuristic tuning and its HIL validation," *Int. Trans. Electr. Energy Syst.*, vol. 30, no. 5, May 2020, Art. no. e12335, doi: 10.1002/2050-7038.12335.

[37] J. P. Bonaldo, J. D. A. Olímpio Filho, A. M. dos Santos Alonso, H. K. M. Paredes, and F. P. Marafão, "Modeling and control of a single-phase grid-connected inverter with LCL filter," *IEEE Latin Amer. Trans.*, vol. 19, no. 2, pp. 250–259, Feb. 2021, doi: 10.1109/TLA.2021.9443067.

[38] *Resolução Normativa*, 414th ed., Aneel, Brazilian Government Ordinance Number 414, Agência Nacional de Energia Elétrica, Sep. 2010.

[39] A. Reznik, M. G. Simões, A. Al-Durra, and S. M. Muyeen, "*LCL* filter design and performance analysis for grid-interconnected systems," *IEEE Trans. Ind. Appl.*, vol. 50, no. 2, pp. 1225–1232, Apr. 2014, doi: 10.1109/TIA.2013.2274612.

[40] S. Buso and P. Mattavelli, *Digital Control in Power Electronics*, 2nd ed. San Rafael, CA, USA: Morgan & Claypool, 2015.

[41] J. P. Bonaldo, H. K. M. Paredes, and J. A. Pomilio, "Control of single-phase power converters connected to low-voltage distorted power systems with variable compensation objectives," *IEEE Trans. Power Electron.*, vol. 31, no. 3, pp. 2039–2052, Mar. 2016, doi: 10.1109/TPEL.2015.2440211.

[42] F. Liu, Y. Zhou, S. Duan, J. Yin, B. Liu, and F. Liu, "Parameter design of a two-current-loop controller used in a grid-connected inverter system with LCL filter," *IEEE Trans. Ind. Electron.*, vol. 56, no. 11, pp. 4483–4491, Nov. 2009, doi: 10.1109/TIE.2009.2021175.
[43] F. P. Marafão, D. I. Brandão, F. A. S. Gonçalves, and H. K. M. Paredes, "Decoupled reference generator for shunt active filters using the conservative power theory," *J. Control, Autom. Electr. Syst.*, vol. 24, no. 4, pp. 522–534, Aug. 2013, doi: 10.1007/s40313-013-0043-0.
[44] R. Teodorescu, F. Blaabjerg, M. Liserre, and P. C. Loh, "Proportional-resonant controllers and filters for grid-connected voltage-source converters," *IEE Proc. Electr. Power Appl.*, vol. 153, no. 5, p. 750, 2006, doi: 10.1049/ip-epa:20060008.
[45] P. Tenti, H. K. M. Paredes, and P. Mattavelli, "Conservative power theory, a framework to approach control and accountability issues in smart microgrids," *IEEE Trans. Power Electron.*, vol. 26, no. 3, pp. 664–673, Mar. 2011, doi: 10.1109/TPEL.2010.2093153.
[46] Y. Ding, M. Mao, and L. Chang, "Conservative power theory and its applications in modern smart grid: Review and prospect," *Appl. Energy*, vol. 303, Dec. 2021, Art. no. 117617, doi: 10.1016/j.apenergy.2021.117617.
[47] H. Akagi, E. H. Watanabe, and M. Aredes, *Instantaneous Power Theory and Applications to Power Conditioning*, 2nd ed. Hoboken, NJ, USA: Wiley, 2017, doi: 10.1002/9781119307181.
[48] F. Zheng Peng, G. W. Ott, and D. J. Adams, "Harmonic and reactive power compensation based on the generalized instantaneous reactive power theory for three-phase four-wire systems," *IEEE Trans. Power Electron.*, vol. 13, no. 6, pp. 1174–1181, Nov. 1998, doi: 10.1109/63.728344.
[49] T. E. Nunez-Zuniga and J. A. Pomilio, "Shunt active power filter synthesizing resistive loads," *IEEE Trans. Power Electron.*, vol. 17, no. 2, pp. 273–278, Mar. 2002, doi: 10.1109/63.988946.

AUGUSTO MATHEUS DOS SANTOS ALONSO (Member, IEEE) received the first Ph.D. degree in electric power engineering from São Paulo State University (UNESP), Brazil, in 2021, and the second Ph.D. degree from the Norwegian University of Science and Technology (NTNU), Norway. In 2015, he was with Whirlpool Latin America/IEL/CNPq as a Research and Development Engineer under the InovaTalentos Fellowship. He was a Postdoctoral Researcher funded by FAPESP with the University of Campinas (UNICAMP), Brazil, until June 2022. He is currently an Assistant Professor with the Department of Electrical and Computer Engineering, University of São Paulo (USP/EESC). His main research interests include digital control of power converters, microgrid control, power quality, and smart grids. He is a member of SOBRAEP. He was a recipient of Brazilian Power Electronics Society (SOBRAEP) Award for the best M.S. dissertation and best Ph.D. thesis of the year, in 2019 and 2022, respectively.

LUIS DE ORO ARENAS received the B.S. degree in electronic engineering from the National University of Colombia, Bogotá, in 2012, and the M.Sc. and Ph.D. degrees in electrical engineering from São Paulo State University (UNESP), in 2014 and 2019, respectively. He conducted a postdoctoral studies with the Power Electronics Laboratory, UNESP/FEIS, in 2019, and the Institute of Science and Technology of Sorocaba, UNESP, from 2020 to 2022. He is currently an Assistant Professor with ICTS, UNESP, affiliated with the Department of Environmental Engineering. His research interests include electronic instrumentation and data science applied to environmental systems, power electronics, power quality, and digital and analog signal processing.

JAKSON PAULO BONALDO received the B.S. degree in electrical engineering from the Federal University of Mato Grosso (UFMT), Cuiabá, Brazil, in 2003, and the M.S. and Ph.D. degrees in electrical engineering from the University of Campinas (UNICAMP), Campinas, Brazil, in 2010 and 2015, respectively. From 2010 to 2011, he was a Firmware Engineer with Padtec Optical Components and Systems. From 2013 to 2018, he was an Assistant Professor with the Federal University of Technology—Paraná (UTFPR). Since 2018, he has been with the Department of Electrical Engineering, UFMT, as an Assistant Professor. His current research interests include power electronics, integration of distributed energy systems, and the control of grid-connected power converters.

JOSE DE A. OLÍMPIO FILHO received the B.S. degree in electrical engineering from the Federal University of Mato Grosso do Sul, Brazil, in 2017, and the M.S. degree in electrical engineering from São Paulo State University (UNESP/FEB), Brazil, in 2019. His main research interests include power electronics and power quality.

FERNANDO PINHABEL MARAFÃO (Member, IEEE) received the B.S. degree in electrical engineering from São Paulo State University (UNESP), Brazil, in 1998, and the M.Sc. and Ph.D. degrees from the University of Campinas (UNICAMP), Brazil, in 2000 and 2004, respectively. In 2002, he joined the Power Electronics Group, University of Padua, Italy, as a Visiting Student. In 2013, he joined Colorado School of Mines, Golden, CO, USA, as a Visiting Scholar on autonomous and intelligent distributed energy systems. Since 2005, he has been an Associate Professor with the Group of Automation and Integrating Systems, UNESP. His current research interests include smart grid technologies, renewable energies, energy management, and power theories. He is a member of Brazilian Power Electronics Society (SOBRAEP) and Brazilian Automation Society (SBA).

HELMO K. MORALES PAREDES (Senior Member, IEEE) received the B.Sc. degree in electrical engineering from San Agustin National University Arequipa, Arequipa, Peru, in 2002, and the M.Sc. and Ph.D. degrees in electrical engineering from the University of Campinas, Campinas, Brazil, in 2006 and 2011, respectively. In 2009, he joined the Power Electronics Group, University of Padova, Italy, as a Visiting Student. In 2014, he joined the PEMC Group, University of Nottingham, U.K., as a Visiting Scholar. In 2018, he joined the ACEPS Group, Colorado School of Mines, Golden, CO, USA, as a Visiting Scholar. Since December 2011, he has been with São Paulo State University (UNESP), Sorocaba, Brazil, where he is currently an Associate Professor and the Leader of the Group of Automation and Integrating Systems (GASI). His current research interests include power quality, power theories, harmonics propagation, power electronics applied to renewable energy systems, and microgrid control. He is a member of Brazilian Power Electronics Society (SOBRAEP) and Brazilian Automation Society (SBA). He received the Prize Paper Award from IEEE TRANSACTIONS ON POWER ELECTRONICS, in 2012, and two consecutive Best Paper Awards from Brazilian Power Quality Society (SBQEE), in 2021 and 2023.